JOC The Journal of Organic Chemistry

Article

Cite This: J. Org. Chem. 2020, 85, 1476−1483

pubs.acs.org/joc

In Situ Cyclization of Proteins (INCYPRO): Cross-Link Derivatization Modulates Protein Stability

Saskia Neubacher,* Jordy M. Saya, Alessia Amore, and Tom N. Grossmann*

Department of Chemistry & Pharmaceutical Sciences, VU University Amsterdam, De Boelelaan 1083, 1081 HV Amsterdam, The Netherlands

Supporting Information

ABSTRACT: Protein macrocyclization represents a very efficient strategy to increase the stability of protein tertiary structures. Here, we describe a panel of novel C3-symmetric tris-electrophilic agents and their use for the cyclization of proteins. These electrophiles are reacted with a protein domain harboring three solvent-exposed cysteine residues, resulting in the in situ cyclization of the protein (INCYPRO). We observe a clear dependency of cross-linking rates on the electrophilicity. All nine obtained cross-linked protein versions show considerably increased thermal stability (up to 29 °C increased melting temperature) when compared to that of the linear precursor. Most interestingly, the degree of stabilization correlates with the hydrophilicity of the cross-link. These results will support the development of novel cross-linked proteins and enable a more rational design process.

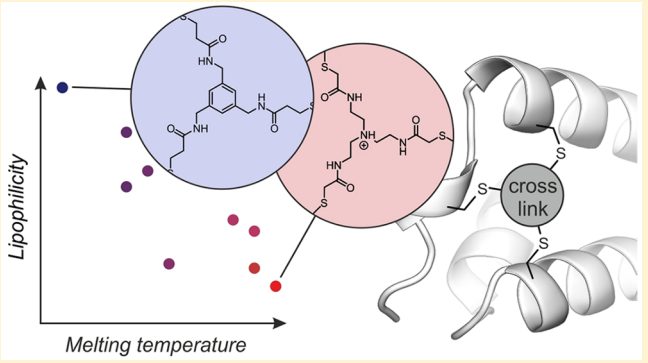

INTRODUCTION

Proteins play a central role in biological processes, and their unique biocatalytic and recognition properties render them attractive for many applications, ranging from medical diagnostics to the synthesis of complex molecular scaffolds.[1,2] Protein function is tightly linked to its three-dimensional structure, which is defined by the primary amino acid sequence and mediated by intramolecular interactions involving both backbone and side-chain atoms. This triggers the formation of secondary structures and allows their assembly into tertiary structures.[3] The use of proteins in biochemical applications can be hampered by the often required harsh conditions, such as increased temperature, leading to loss of protein tertiary structure and therefore functionality. Various approaches have been developed that facilitate the stabilization of protein tertiary structures involving sequence variation through consensus-based mutagenesis, directed evolution, computational approaches, and/or the introduction of nonproteinogenic amino acids.[4−8] Notably, macrocyclization strategies also proved effective in stabilizing protein folds as the resulting covalent intradomain cross-links impede the opening of the tertiary structure.[9−15]

A large repertoire of macrocyclization reactions is available for peptides and small proteins that are accessible via total chemical synthesis, allowing the incorporation of a variety of functional groups.[16,17] For proteins that are obtained via heterologous expression, only a limited set of macrocyclization reactions has been reported, including the introduction of disulfides,[18] disulfide mimics,[9] or lactam formation.[10−12] To circumvent the structural prerequisites associated with these approaches, electrophilic non-natural amino acids have been introduced into proteins to react with the thiol group of an appropriately aligned cysteine residue.[13,14] We recently reported a novel approach involving the in situ cyclization of proteins (INCYPRO, Figure 1a), where we aimed to maximize the stabilization effect from cross-linking while circumventing the complications associated with protein expression using non-natural amino acids.[19] INCYPRO involves the introduction of three spatially aligned cysteines that are located in different secondary structure elements of the protein. The three cysteine thiol groups are then reacted with a C3-symmetric, tris-electrophilic agent composed of a central core structure (X) that projects three electrophilic groups (El, Figure 1a). When starting from a linear protein precursor, the reaction provides a protein with bicyclic topology. At ambient temperatures, cross-link introduction did not alter the protein function. Importantly, cross-linking conveyed increased stability toward thermal and chemical stress.[19] So far, only chloroacetamide-modified tertiary amine core structures were employed, and it is unclear how variation of the tris-electrophile affects modification efficiencies and protein stability.

Herein, we report the synthesis and characterization of structurally diverse tris-electrophiles suitable for cross-linking native proteins. We further investigate how derivatization effects cross-linking reactivity and the stability of the resulting

Special Issue: Modern Peptide and Protein Chemistry

Received: September 13, 2019
Published: December 2, 2019

DOI: 10.1021/acs.joc.9b02490
J. Org. Chem. 2020, 85, 1476−1483

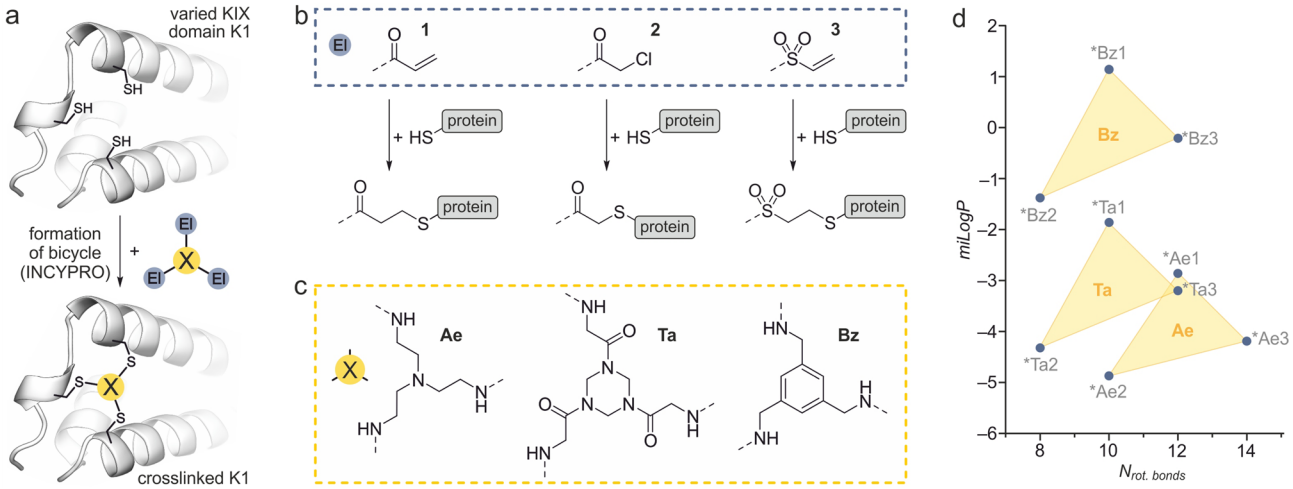

Figure 1. (a) Concept of the in situ cyclization of proteins (INCYPRO) using triple cysteine variant of the KIX domain, **K1** (aa 586−671, H594C, L599C, R646C). Reaction occurs between the three introduced thiol groups in **K1** and a C3-symmetric core structure (X) decorated with three electrophilic groups (El). (b) Used electrophilic groups (El, **1**, **2**, and **3**) and the resulting cross-linked products after reaction with a protein-exposed thiol. (c) C3-symmetric core structures **Ae**, **Ta**, and **Bz**. (d) Lipophilicity (*miLogP*)[20] and flexibility ($N_{\text{rot. bond}}$: number of rotatable bonds between two thiol groups) were calculated (for details, see Scheme 1) and plotted.

Scheme 1. Overview of the Nine Cross-Link Structures That Result from the Reaction of the Tris-Electrophiles with Three Thiol Groups[a]

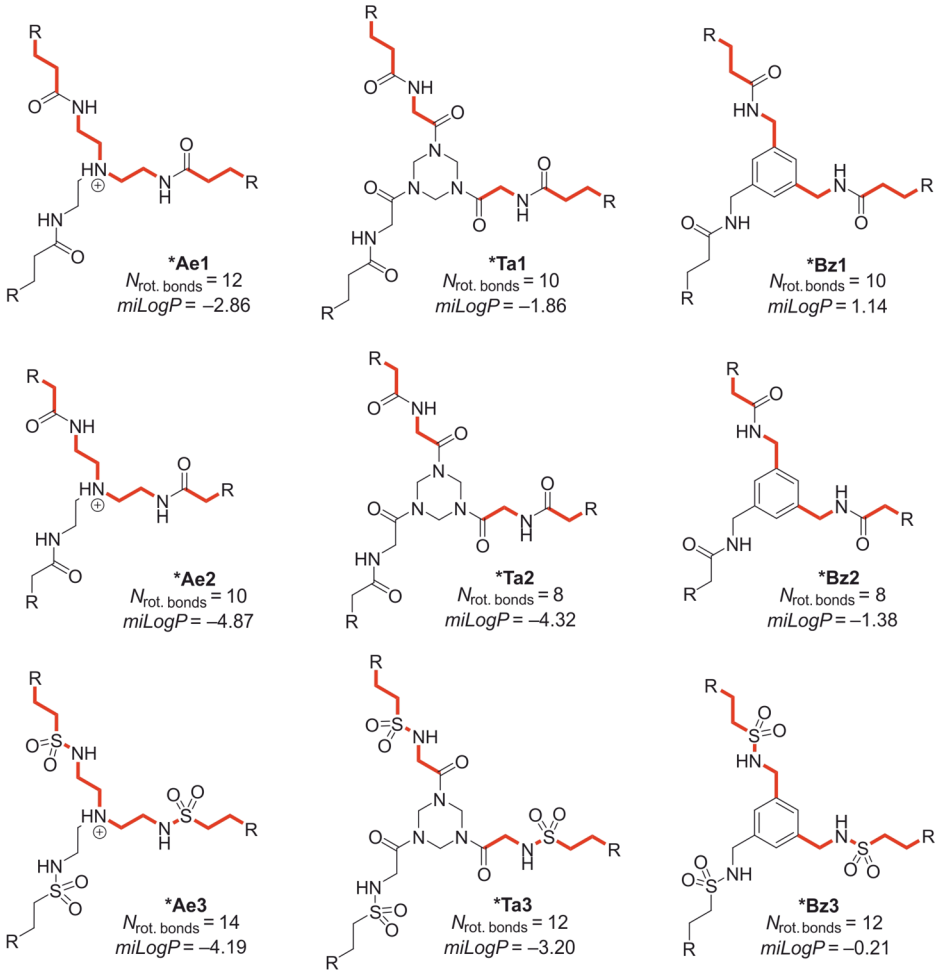

[a]The number of rotatable bonds ($N_{\text{rot. bonds}}$) was determined for the shortest chain between two thioether moieties (R = S-protein). Rotatable bonds are highlighted in red. For calculation of *miLogP* values, structures were considered as depicted (R = H). For calculations, Molinspiration was used.[20]

DOI: 10.1021/acs.joc.9b02490
J. Org. Chem. 2020, 85, 1476−1483

bicyclic protein. In total, nine structurally distinct cross-links were designed and their corresponding tris-electrophiles synthesized. Subsequently, their reaction with the KIX protein domain containing three appropriately positioned cysteines (**K1**) was investigated.

RESULTS AND DISCUSSION

Design of Tris-Electrophilic Agents. We selected acrylamide (**1**), chloroacetamide (**2**), and vinyl sulfonamide (**3**, Figure 1b) as reactive groups to utilize their distinct electrophilicities (**1** < **2** < **3**).[21,22] In addition, three different core structures, based on triethylamine (**Ae**), triazinane (**Ta**), and benzene (**Bz**),[23] were chosen. These structures possess a C3-symmetric geometry and bear three amino groups to enable the functionalization with the electrophiles (Figure 1c). The combination of the three electrophiles (**1**–**3**) with the three core structures (**Ae**, **Ta**, **Bz**) results in nine different tris-electrophilic reagents (Figure S1), which upon cross-linking with the three cysteines in protein **K1** results in nine structurally diverse cross-links (indicated by *, Scheme 1). We expected these cross-links to exhibit distinct physicochemical properties and decided to focus on flexibility and hydrophobicity as two very important characteristics.[24] Based on a classification usually applied for the characterization of bioactive small molecules, we used the number of rotatable bonds ($N_{\text{rot. bonds}}$) as a measure for flexibility. Here, we considered the shortest chain between two of the thioether moieties (red = rotatable bond, Scheme 1) using the isolated cross-link as a basis. Overall, the number of rotatable bonds ranges from eight (***Ta2** and ***Bz2**) to 14 (***Ae3**). To estimate cross-link lipophilicity, we calculated *miLogP* values, which show a broad distribution for our set of cross-links ranging from rather hydrophobic (***Bz1**: *miLogP* = 1.14) to relatively polar structures (***Ae2**: *miLogP* = −4.87, Scheme 1). In these calculations, the triethylamine core (**Ae**) was presumed to be protonated as we were interested in these properties at neutral pH (R_3NH^+, ca. pK_a 9). When plotting $N_{\text{rot. bond}}$ against *miLogP* values for all cross-links (Figure 1d), we observe a relatively broad and even distribution of both characteristics within our cross-link library. Notably, both the core structure and the reacted electrophilic moiety add to the overall cross-link diversity.

Amidation Reactions of Triamine Cores. For the assembly of the desired tris-electrophilic molecules, we aimed for tris-amino-functionalized cores (**4**–**6**) as precursors that could be functionalized via (sulfon)amide formation (Scheme 2). The tris-amino version of the **Ae** core (**4**) is commercially available, whereas the corresponding derivative of **Bz** (**6**) is readily accessible following literature procedures.[25,26] The tris-amino derivative of the **Ta** core (**5**) was synthesized in good yields, starting from tribromide **7**[27] via an azide substitution reaction yielding triazide **8** and a subsequent catalytic hydrogenation in 82 and 70% yield, respectively. With tris-amino-functionalized cores **4**–**6** in hand, we proceeded with the coupling of electrophilic moieties (**1**–**3**) using acid chlorides **9** and **10** and sulfonyl chloride **11**. Such reactions have been reported to typically result in low yields due to both competing polymerization reactions between unreacted amine and the attached electrophile and intramolecular reactions.[28,29] For the synthesis of acrylamide-modified cores (**Ae1**, **Ta1**, **Bz1**), tris-amino-functionalized molecules **4**–**6** were reacted with acryloyl chloride (**9**) using an excess of inorganic base in a mixture of water and organic solvent. For **Bz1**, the yields were

Scheme 2. (a) Synthesis of Tris-Amino-Functionalized Core Ta (5) and (b) Synthesis of Tris-Electrophilic Agents Ae1–3, Ta1–3, and Bz1–3 Starting from Their Tris-Amino Precursors (4–6)

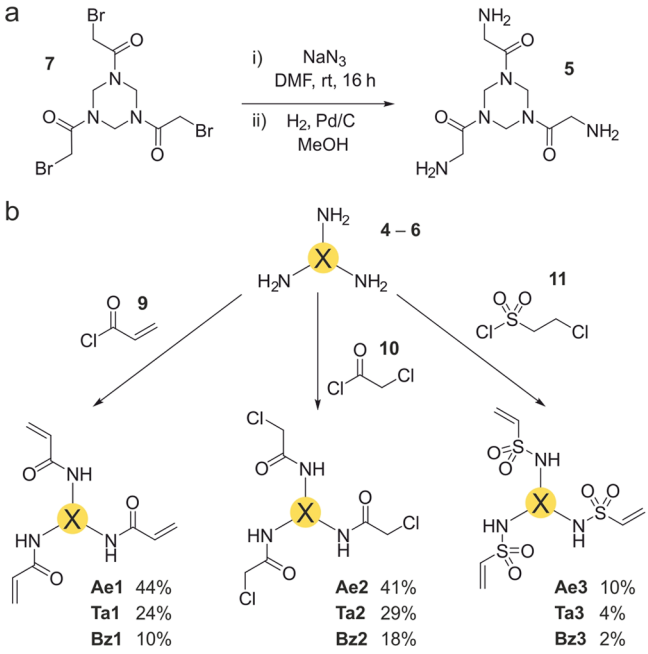

relatively low (10%) when compared to those of **Ae1** (44%) and **Ta1** (24%), mainly due to the poor solubility. Using a similar procedure, tris-chloroacetamides (**Ae2**, **Ta2**, **Bz2**) were synthesized in yields ranging from 18 to 41%. For the synthesis of vinyl sulfonamides (**Ae3**, **Ta3**, **Bz3**), a different protocol was applied (i.e., Et_3N, DCM, −60 °C to rt)[21] using 2-chloroethanesulfonyl chloride (**11**). In these cases, yields were generally low due to more pronounced polymerization reactions caused by the high electrophilicity of the vinyl sulfonamides. All tris-electrophilic agents were isolated in good purity and sufficient quantities for in situ cyclization with **K1**.

In Situ Cyclization of Protein K1. The triple-cysteine variant of the KIX domain, **K1** (aa 586–671, H594C, L599C, R646C) previously applied to establish the INCYPRO approach, was used as a model protein. Initially, the reactions between **K1** and the three tris-electrophilic **Ae** cores (**Ae1**, **Ae2**, **Ae3**) were performed at pH 8.5 following the original protocol.[19] High-performance liquid chromatography in combination with mass spectrometry (HPLC–MS) clearly indicated the formation of the cross-linked proteins (Figure 2a) and verified the expected reactivity trend (**Ae1** < **Ae2** < **Ae3**). Adjusted reaction conditions (Table S1) facilitated quantitative conversion in all three cases, as confirmed by HPLC–MS (Figure 2b). Encouraged by these results, we reacted all tris-electrophiles with **K1** at three different pH values (8.5, 7.5, 6.5) taking samples after 1, 3, and 5 h (Figures S2–S4). The heat map representation of these measurements (Figure 2c) reveals similar reactivity trends for all three cores, showing slower conversion with reduced electrophilicity (**3** > **2** > **1**). Not surprisingly, overall reactivity decreases with decreasing pH owing to a reduced nucleophilicity of the thiol groups. Nevertheless, for all vinyl sulfonamide (**3**)-based tris-electrophiles, we observed considerable product formation even at pH 6.5. Under individually optimized reaction conditions (Table S1), we were able to obtain full conversion

DOI: 10.1021/acs.joc.9b02490
J. Org. Chem. 2020, 85, 1476–1483

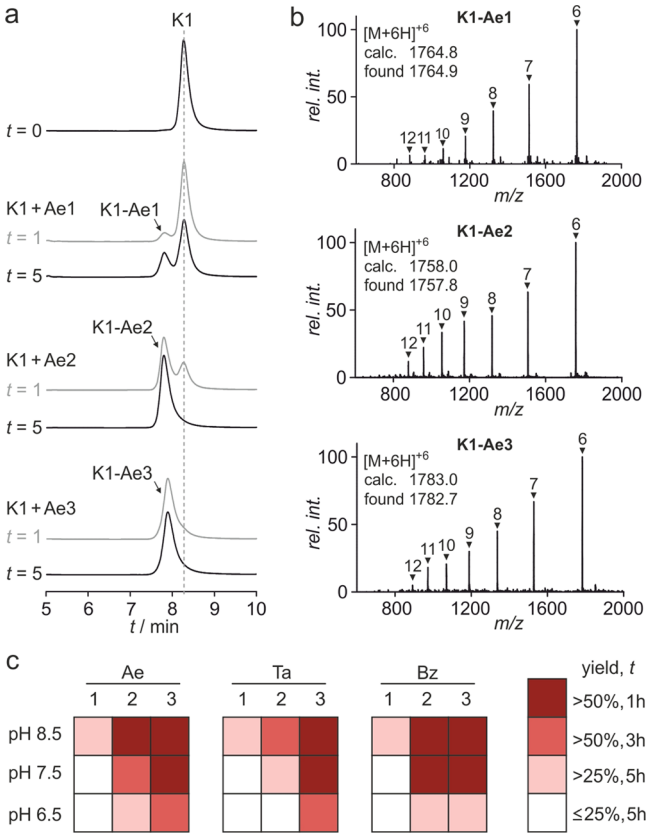

Figure 2. (a) HPLC chromatograms of reactions between **K1** and **Ae1**, **Ae2**, and **Ae3** (pH 8.5, 25 °C, after 1 and 5 h). (b) Electrospray ionization (ESI) mass spectra of cross-linked **K1**. (c) Heat map representation of reaction yield, allowing a comparison of relative reaction rates (analytical yields are based on HPLC chromatograms, Figures S2–S4).

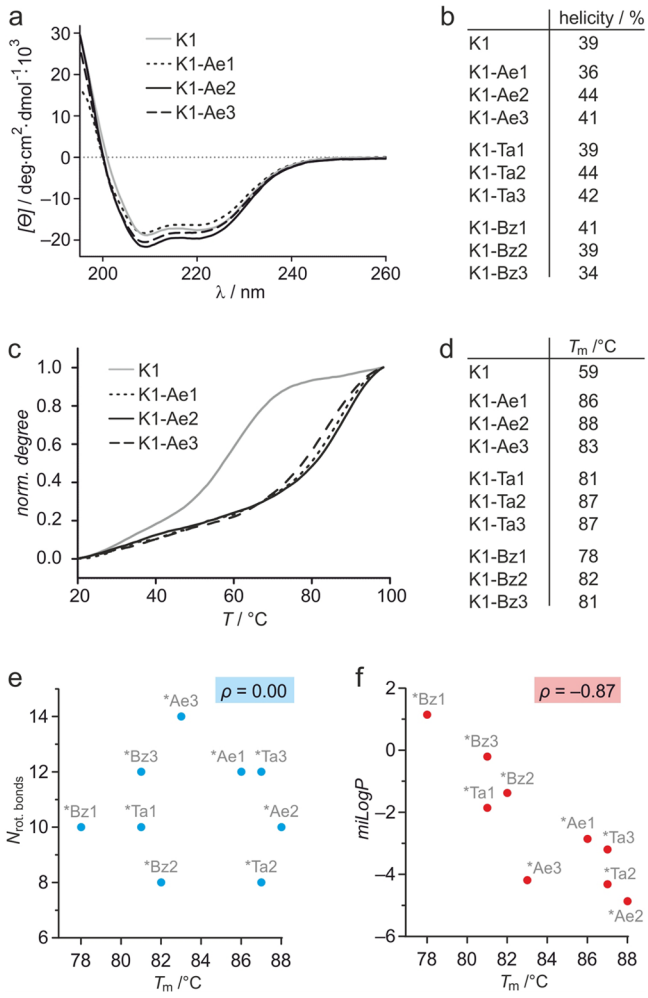

Figure 3. (a) CD spectra of **K1**, and cross-linked **K1-Ae1**, **K1-Ae2**, and **K1-Ae3** are shown in molar ellipticity [θ]. (b) Overview of calculated helicities based on the CD signal at λ = 222 nm (for spectra of **Ta**- and **Bz**-cross-linked **K1**, see Figures S17 and S18). (c) Thermal denaturation curves of **K1** and cross-linked **K1-Ae1**, **K1-Ae2**, and **K1-Ae3**. The CD signal was recorded at λ = 222 nm as a function of temperature. (d) Overview of T_m values derived from the corresponding thermal denaturation curves (Figures S19 and S20). (e) Number of rotatable bonds between two thioether groups ($N_{rot.\ bonds}$) vs melting temperatures (T_m), including the resulting Pearson correlation coefficient (ρ). (f) Calculated *miLogP* values vs melting temperatures (T_m), including the resulting Pearson correlation coefficient (ρ).

for all tris-electrophiles (Figures S5–S13). Importantly, we did not observe any protein multimerization, which indicates that the first nucleophilic attack is the rate-limiting step and is in agreement with our previous study.[19] For chloroacetamide-based electrophiles **Ae2**, **Ta2**, and **Bz2**, loss of the three Cl atoms verifies the reaction with all three cysteines in **K1**. In these cases, we did not observe any partially reacted tris-electrophiles, indicating that after a first reaction, the subsequent two intramolecular reactions proceed rapidly, presumably due to increased effective concentrations. We expect an analogous behavior for acrylamide- and vinylsulfonamide-based electrophiles, but our MS data are not suitable for verification because intramolecular addition reactions do not change the overall molecular weight. To probe for free cysteines, **K1**, **K1-Bz1**, and **K1-Bz3** were incubated with an excess of iodoacetamide, which selectively alkylates free thiols. As expected, **K1** was quantitatively converted into the tris-alkylated product (Figure S16). Importantly, we do not observe any alkylation for **K1-Bz1** and **K1-Bz3**, indicating the absence of unreacted cysteines (Figure S16).

Thermal Stability of Cross-Linked K1. The KIX domain has been structurally characterized, revealing three central α-helices as the core secondary structure elements (Figure 1a).[30] To assess the structural properties of our cross-linked variants, we performed circular dichroism (CD) spectroscopy. As expected, the CD spectrum of **K1** shows the two minima around λ = 210 and 222 nm (Figure 3a), indicative of the presence of α-helices. Based on the signal at 222 nm, a helical content of 39% was determined that lies in the expected range.[30,31] We then measured the CD spectra of all cross-linked **K1** derivatives showing analogous characteristics (Figure 3a and Figures S17 and S18). Consequently, all cross-linked **K1** versions exhibit similar helicities ranging from 34 to 44%. This indicates that the different cross-links do not impact the overall structure of **K1**. Subsequently, we measured the temperature dependence of the CD signal at λ = 222 nm, providing melting curves (Figure 3c and Figures S19 and S20) that allow the determination of the melting temperatures (T_m). For all cross-linked **K1** derivatives, we observe a melting temperature higher than that for the linear precursor **K1** (Figure 3d). Differences in T_m values range from 19 °C for **K1**-

DOI: 10.1021/acs.joc.9b02490
J. Org. Chem. 2020, 85, 1476–1483

Bz1 (T_m = 78 °C) to 29 °C for **K1-Ae2** (T_m = 88 °C) when compared to that of **K1** (T_m = 59 °C), indicating that individual cross-links result in a different degree of thermal stabilization.

Having initially calculated parameters indicative of cross-link flexibility and hydrophobicity (Figure 1d and Scheme 1), we were interested if there is any correlation of these parameters with the thermal stability of the cross-linked proteins. Therefore, we plotted the number of rotatable cross-link bonds between two of the formed thioethers ($N_{rot.\ bond}$, Scheme 1) against the determined T_m values and determined a Pearson correlation coefficient of $\rho = 0$ (Figure 3e). Values of ρ can range between −1 and 1, with the value 0 indicating the absence of any correlation. The lack of correlation between thermal stability (T_m) and flexibly ($N_{rot\ bonds}$) in our data set is also highlighted by the fact that the most stable protein **K1-Ae2** (T_m = 88 °C) and the cross-linked protein with the lowest stability **K1-Bz1** (T_m = 78 °C) possess the same number of rotatable cross-link bonds ($N_{rot\ bonds}$ = 10). On the other hand, a plot of T_m values against calculated *miLogP*, which is a measure for lipophilicity, shows a clear correlation of ρ = −0.87 (Figure 3f). Here, the most lipophilic cross-link, ***Bz1** (*miLogP* = 1.14), can be found in the least stable cross-linked protein, **K1-Bz1** (T_m = 78 °C), whereas the most stable protein, **K1-Ae1** (T_m = 88 °C), harbors the most hydrophilic cross-link, ***Ae1** (*miLogP* = −4.87). In general, we observe a lower degree of stabilization for the most hydrophobic benzene-derived core **Bz**, whereas both relatively polar core structures **Ae** and **Ta** contribute more to stability. In addition, it is interesting to note that the most hydrophilic thioether moiety originating from the reaction of chloroacetamide (**2**) is for each core the most stable derivative (**Ae2**, **Bz2**, and **Ta2**, for the latter together with **Ta3**).

CONCLUSIONS

We report the synthesis of a panel of nine tris-electrophiles (Figure S1) originating from a combination of three core structures (**Ae**, **Ta**, and **Bz**) and three electrophilic moieties (**1**−**3**). Among these tris-electrophiles, only **Ae2** has been previously reported.[19] The final step in the synthesis of reagents containing acrylamide (**1**) and chloroacetamide (**2**) involved amide bond formation between tris-amino cores (**4**−**6**) and acid chloride derivatives (**9** and **10**, Scheme 2). For vinyl sulfonamide (**3**)-containing products, the tris-amino cores (**4**−**6**) were reacted with 2-chloroethanesulfonyl chloride (**11**). As previously reported, these (sulfone)amide formations proceeded with only low to moderate yields, mainly owing to undesired inter- and intramolecular reaction of unreacted amines with already coupled electrophilic groups.[28,29] For this reason, the most reactive vinyl-sulfonamide-modified cores (**Ae3**, **Ta3**, and **Bz3**) were obtained with lowest yields (2−10%).

All tris-electrophiles were obtained in good purities suitable for the cross-linking of protein **K1**. Protein **K1** comprises 88 amino acids and possesses three cysteine residues appropriately aligned for the reaction with our tris-electrophilic agents. The reaction between **K1** and **Ae2** yields bicyclic protein **K1-Ae2** and had been previously described by us.[19] In addition to chloroacetamide (**2**), we selected acrylamide (**1**) and vinyl sulfonamide (**3**) which, in aqueous solution, are more and less electrophilic, respectively. The cross-linking reactions were performed in buffered solution at three different pH values (6.5, 7.5, and 8.5, T = 25 °C). At pH 8.5, we observed product formation for all tris-electrophiles including the least reactive ones bearing the acrylamide (**1**, Figure 2C). As expected, conversion to cross-linked **K1** becomes slower with decreasing pH values. Most notably, even at pH 6.5 and only 5 h reaction time, we observed more than 50% product formation for all vinyl sulfonamide (**3**)-containing cores (**Ae3**, **Ta3**, **Bz**, Figures S2−S4). This is a remarkable finding as it broadens the applicability of the INCYPRO approach to proteins that are either not stable or soluble at higher pH values.

Using individually optimized reaction conditions (Table S1), we obtained all cross-linked **K1** versions as confirmed by MS (Figures S5−S13). CD spectroscopy indicates a similar helical content for all cross-linked proteins (34−44%), which was in the range of the linear precursor **K1** (39%, Figure 3b), suggesting that cross-linking does not interfere with the overall protein structure. When determining the thermal stability using CD melting experiments, all cross-linked **K1** proteins showed considerably increased melting temperatures (T_m = 78−88 °C) when compared to linear **K1** (T_m = 59 °C, Figure 3d). A clear dependency between thermal stabilization of the modified protein and lipophilicity of the introduced cross-link can be observed and results in a very good correlation coefficient (T_m vs *miLogP*: ρ = −0.87). This indicates that protein stability particularly benefits from cross-links with hydrophilic structures, which is supported by findings from protein surface engineering showing that increasing the overall polarity of the protein surface increases protein stability, presumably due to a reduced tendency for aggregation.[7] The opposite is the case for the introduction of hydrophobic solvent-exposed residues. However, it remains to be seen if the stability trends observed for **K1** are also generally applicable for other proteins.

Taken together, we report novel tris-electrophilic molecules suitable for protein cross-linking using the in situ cyclization of proteins (INCYPRO) approach. These molecules vary in their electrophilicity, thereby broadening the accessible pH range, for example, potentially enabling the cross-linking of proteins that are not stable under basic conditions. Most notably, all nine cross-linked versions of **K1** showed considerably increased thermal stability ($\Delta T_m \geq 19$ °C), and it appears that the degree of stabilization is more pronounced when hydrophilic cross-links are attached. These findings will support the future development of cross-linked proteins and enable a more rational design process.

EXPERIMENTAL SECTION

General Methods. Unless stated otherwise, all solvents and commercially available reagents were used as purchased. Benzene-1,3,5-triyltrimethanamine (**6**) and 1,1′,1″-(1,3,5-triazinane-1,3,5-triyl)tris(2-bromoethan-1-one) (**7**) were synthesized according to literature procedures.[25−27] Unless stated otherwise, all solvents and commercially available reagents were used as purchased. Nuclear magnetic resonance (NMR) spectra were recorded on a Bruker AVANCE 600 MHz (150.92 MHz for ^{13}C), Bruker AVANCE 500 MHz (125.78 MHz for ^{13}C), or Bruker AVANCE 300 MHz (83.85 MHz for ^{13}C) as indicated below. The residual solvent was used as an internal standard (^1H, δ 7.26 ppm; $^{13}C\{^1H\}$, δ 77.16 ppm for $CDCl_3$; ^1H, δ 2.50 ppm; $^{13}C\{1H\}$, δ 39.52 ppm for DMSO-d_6). Chemical shifts (δ) are given in parts per million (ppm), and coupling constants (J) are quoted in hertz (Hz). Resonances are described as s (singlet), d (doublet), t (triplet), q (quartet), quint (quintet), sex (sextet), sep (septet), br (broad singlet), and m (multiplet) or combinations thereof. Infrared (IR) spectra were recorded neat using a Shimadzu FTIR-8400s spectrophotometer, and wavelengths are reported in cm^{-1}. Electrospray ionization (ESI) high-resolution mass spectrometry (HRMS) was carried out using a Bruker microTOF-Q instrument

DOI: 10.1021/acs.joc.9b02490
J. Org. Chem. 2020, 85, 1476−1483

in positive ion mode (capillary potential of 4500 V). Flash chromatography was performed manually on Silicycle Silia-P flash silica gel (particle size 40−63 μm, pore diameter 60 Å) using the indicated eluent. Reversed-phase chromatography was performed using a Biotage Isolera equipment using Biotage SNAP cartridges or an Xbridge prep (C18) 5 μm column (19 mm × 100 mm). Thin layer chromatography (TLC) was performed using TLC plates from Merck (SiO_2, Kieselgel 60 F254 neutral, on aluminum with fluorescence indicator), and compounds were visualized by UV detection (254 nm) and $KMnO_4$ stain. Mass spectrometry analyses were performed using a Shimadzu LCMS-2020 mass spectrometer. The data were acquired in full-scan APCI mode (MS) from m/z 100 to 800 in positive ionization mode. Data were processed using Shimadzu Labsolutions 5.82. Protein and cross-linker identity and purity were confirmed by HPLC/ESI-MS analysis performed in a HPLC-MS system (Agilent Technologies) provided with a Zorbax Eclipse, XDB-C18 reverse-phase column (4.6 × 150 mm, particle size 5 μm, Agilent; solvent A: H_2O + 0.1% TFA; solvent B: acetonitrile +0.1% TFA; flow rate of 1 mL min^{-1}).

*1,1′,1″-(1,3,5-Triazinane-1,3,5-triyl)tris(2-azidoethan-1-one) (**8**).* To a solution of sodium azide (1.25 g, 19.2 mmol, 3.2 equiv) in DMF (100 mL) was added 1,1′,1″-(1,3,5-triazinane-1,3,5-triyl)tris(2-bromoethan-1-one) (**7**, 2.7 g, 6 mmol, 1 equiv), and the solution was stirred for 40 h at room temperature. After full consumption of the starting material, water was added and the product was extracted with EtOAc. The combined organic layers were washed with brine, dried over Na_2SO_4, and concentrated in vacuo. The crude mixture was purified by flash chromatography using EtOAc/cyclohexane (3:1) as eluent to obtain the product as a white amorphous solid (1.65 g, 4.91 mmol, 82%): R_f = 0.15 (EtOAc/cyclohexane 3:1); ^{1}H NMR (500 MHz, DMSO-d_6) δ 5.16 (s, 6H), 4.27 (s, 6H); ^{13}C NMR (126 MHz, DMSO-d_6) δ 167.3 (3C), 55.0 (3C), 49.6 (3C); IR (neat) ν_{max} (cm^{-1}) = 2104, 1649, 1413, 1236, 947; HRMS-ESI (m/z) [M + H]$^+$ calcd for $C_9H_{13}N_{12}O_3$, 337.1228; found, 337.1228.

*1,1′,1″-(1,3,5-Triazinane-1,3,5-triyl)tris(2-aminoethan-1-one) (**5**).* To a solution of 1,1′,1″-(1,3,5-triazinane-1,3,5-triyl)tris(2-azidoethan-1-one) (**8**, 1 g, 2.97 mmol, 1.0 equiv) in MeOH (20 mL) and DMF (5 mL) was added Pd/C (10 wt %, 319 mg, 0.3 mmol). Hydrogen gas was added via a balloon under atmospheric pressure. TLC showed complete conversion of the starting material after 1 h. The suspension was filtered over Celite and concentrated in vacuo to obtain the product as a white amorphous solid (530 mg, 2.05 mmol, 70%): ^{1}H NMR (500 MHz, DMSO-d_6) δ 5.21 (s, 6H), 3.49 (s, 6H); ^{13}C NMR (126 MHz, DMSO-d_6) δ 172.5 (3C), 54.9 (3C), 43.5 (3C); IR (neat) ν_{max} (cm^{-1}) = 3367, 1647, 1610, 1490, 1200, 845; HRMS-ESI (m/z) [M + H]$^+$ calcd for $C_9H_{19}N_6O_3$, 259.1513; found, 259.1526.

General Procedure A. To a solution of triamine **4**−**6** (1.0 equiv) in CH_2Cl_2(1 M) was added K_2CO_3 (5.0 equiv, 6 M) in H_2O at 0 °C. Upon vigorous stirring, acid chloride (3.3 equiv) was dropwise added, and the mixture was allowed to stir at room temperature overnight. The mixture was diluted with water and extracted three times with CH_2Cl_2. Subsequently, the organic layer was washed with brine, dried over Na_2SO_4, and concentrated in vacuo. The crude was further purified by silica gel column chromatography.

General Procedure B. To a solution of 2-chloroethanesulfonyl chloride (3.3 equiv) in CH_2Cl_2 (1.0 M) was added triethylamine (3.6 equiv) at −60 °C. After being stirred for 2 h, a solution of triamines **4**−**6** (1.0 equiv) and triethylamine (3.3 equiv) in CH_2Cl_2 (0.5 M) was dropwise added, after which the temperature was allowed to slowly increase to room temperature over 16 h. Next, the suspension was filtered and quenched in cold HCl (0.1 M). The product was extracted with CH_2Cl_2, dried over Na_2SO_4, and concentrated in vacuo. The crude was further purified by silica gel column chromatography.

*N,N′,N″-(Nitrilotris(ethane-2,1-diyl))triacrylamide (**Ae1**).* Prepared according to general procedure A using tris(2-aminoethyl)-amine (**4**, 1.5 mL, 10 mmol), K_2CO_3 (6.84 g, 49.5 mmol), and acryloyl chloride (2.67 mL, 33 mmol). The title compound was isolated without purification as a white amorphous solid (1.36 g, 4.4 mmol, 44%): ^{1}H NMR (500 MHz, DMSO-d_6) δ 8.01 (d, J = 5.6 Hz, 3H), 6.25 (dd, J = 17.1, 10.2 Hz, 3H), 6.07 (dd, J = 17.1, 2.2 Hz, 3H), 5.57 (dd, J = 10.2, 2.2 Hz, 3H), 3.17 (q, J = 6.3 Hz, 6H), 2.53 (t, J = 6.6 Hz, 6H); ^{13}C NMR (126 MHz, DMSO-d_6) δ 164.2 (3C), 131.8 (3C), 126.3 (3C), 53.3 (3C), 37.0 (3C); IR (neat) ν_{max} (cm^{-1}) = 3209, 1650, 1614, 1408, 1240, 1171, 955; HRMS-ESI (m/z) [M + H]$^+$ calcd for $C_{15}H_{25}N_4O_3$, 309.1921; found, 309.1941.

*N,N′,N″-(Nitrilotris(ethane-2,1-diyl))tris(2-chloroacetamide) (**Ae2**).* Prepared according to general procedure A using tris(2-aminoethyl)amine (**4**, 1.5 mL, 10 mmol), K_2CO_3 (6.84 g, 49.5 mmol), and chloroacetyl chloride (2.63 mL, 33 mmol). The title compound was isolated without purification as a white amorphous solid (1.55 g, 4.1 mmol, 41%): ^{1}H NMR (600 MHz, DMSO-d_6) δ 8.08 (t, J = 5.6 Hz, 3H), 4.06 (s, 6H), 3.14 (q, J = 6.3 Hz, 6H), 2.52 (t, J = 6.7 Hz, 6H); ^{13}C NMR (151 MHz, DMSO-d_6) δ 166.1 (3C), 52.9 (3C), 42.7 (3C), 37.4 (3C); IR (neat) ν_{max} (cm^{-1}) = 3246, 1654, 1545, 1431, 1171; HRMS-ESI (m/z) [M + H]$^+$ calcd for $C_{12}H_{22}Cl_3N_4O_3$, 375.0752; found, 375.0765.

*N,N′,N″-(Nitrilotris(ethane-2,1-diyl))triethenesulfonamide (**Ae3**).* Prepared according to general procedure B with a cross-linker by treating a solution of 2-chloroethanesulfonyl chloride (236 μL, 2.26 mmol) and triethylamine (338 μL, 2.47 mmol) in CH_2Cl_2 (3 mL) with a solution of tris(2-aminoethyl)amine (**4**, 103 μL, 0.69 mmol) and triethylamine (310 μL, 2.26 mmol) in CH_2Cl_2 (2 mL). The crude was purified by C18 reversed-phase column chromatography to obtain the title compound as a viscous oil (28 mg, 0.067 mmol, 10%): ^{1}H NMR (500 MHz, DMSO-d_6) δ 7.10 (t, J = 5.8 Hz, 3H), 6.72 (dd, J = 16.5, 10.0 Hz, 3H), 6.05 (d, J = 16.5 Hz, 3H), 6.00 (d, J = 9.9 Hz, 3H), 2.87 (q, J = 6.0 Hz, 6H), 2.48 (t, J = 6.1 Hz, 6H); ^{13}C NMR (126 MHz, DMSO-d_6) δ 136.8 (3C), 125.8 (3C), 53.5 (3C), 40.3 (3C); IR (neat) ν_{max} (cm^{-1}) = 3196, 1651, 1614, 1547, 1240, 955; HRMS-ESI (m/z) [M + H]$^+$ calcd for $C_{12}H_{25}N_4O_6S_3$, 417.0931; found, 417.0949.

*N,N′,N″-((1,3,5-Triazinane-1,3,5-triyl)tris(2-oxoethane-2,1-diyl))-triacrylamide (**Ta1**).* Prepared according to general procedure A using 1,1′,1″-(1,3,5-triazinane-1,3,5-triyl)tris(2-aminoethan-1-one) (**5**, 50 mg, 0.19 mmol), K_2CO_3 (173 mg, 1.26 mmol, 6.6 equiv), and acryloyl chloride (51 μL, 0.63 mmol). The crude was purified by C18 reversed-phase column chromatography to obtain the title compound as a white amorphous solid (19 mg, 0.045 mmol, 24%): ^{1}H NMR (500 MHz, DMSO-d_6) δ 8.33 (s, 3H), 6.33 (dd, J = 17.1, 10.2 Hz, 3H), 6.09 (dd, J = 17.1, 2.1 Hz, 3H), 5.62 (dd, J = 10.2, 2.1 Hz, 3H), 5.30 (s, 6H), 4.23 (d, J = 5.5 Hz, 6H); ^{13}C NMR (126 MHz, DMSO-d_6) δ 168.7 (3C), 164.5 (3C), 132.5 (3C), 125.8 (3C), 57.0 (3C), 40.8 (3C); IR (neat) ν_{max} (cm^{-1}) = 3275, 1649, 1535, 1408, 1240, 1194, 945; HRMS-ESI (m/z) [M + H]$^+$ calcd for $C_{18}H_{25}N_6O_6$, 421.1830; found, 421.1847.

*N,N′,N″-((1,3,5-Triazinane-1,3,5-triyl)tris(2-oxoethane-2,1-diyl))-tris(2-chloroacetamide) (**Ta2**).* Prepared according to general procedure A using 1,1′,1″-(1,3,5-triazinane-1,3,5-triyl)tris(2-amino-ethan-1-one) (**5**, 50 mg, 0.19 mmol), K_2CO_3 (173 mg, 1.26 mmol, 6.6 equiv), and chloroacetyl chloride (62 μL, 0.63 mmol). The crude was purified by C18 reversed-phase column chromatography to obtain the title compound as a white amorphous solid (27 mg, 0.055 mmol, 29%): ^{1}H NMR (600 MHz, DMSO-d_6) δ 8.37 (s, 3H), 5.28 (s, 6H), 4.20 (s, 6H), 4.15 (s, 6H); ^{13}C NMR (126 MHz, DMSO) δ 167.7 (3C), 166.2 (3C), 55.2 (3C), 42.4 (3C), 40.8 (3C); IR (neat) ν_{max} (cm^{-1}) = 3272, 1649, 1626, 1535, 1407, 1240, 1171, 926; HRMS-ESI (m/z) [M + H]$^+$ calcd for $C_{15}H_{22}Cl_3N_6O_6$, 487.0661; found, 487.0685.

*N,N′,N″-((1,3,5-Triazinane-1,3,5-triyl)tris(2-oxoethane-2,1-diyl))-triethenesulfonamide (**Ta3**).* Prepared according to a modified general procedure B by treating a solution of 2-chloroethanesulfonyl chloride (91 μL, 0.87 mmol) and triethylamine (130 μL, 0.83 mmol) in MeCN (1 mL) at −30 °C with a solution of 1,1′,1″-(1,3,5-triazinane-1,3,5-triyl)tris(2-aminoethan-1-one) (**5**, 59 mg, 0.23 mmol) and triethylamine (103 μL, 0.76 mmol) in DMSO/H_2O (2:1, 1.5 mL). The reaction was stopped by pouring it into cold MeCN/water (1:1, with 0.1% formic acid). The crude was lyophilized and thereafter purified by C18 reversed-phase column chromatog-

DOI: 10.1021/acs.joc.9b02490
J. Org. Chem. 2020, 85, 1476−1483

raphy to obtain the title compound as a white foamy solid (5 mg, 9.5 μmol, 4%): ^{1}H NMR (600 MHz, DMSO-d_6) δ 7.56 (s, 3H), 6.67 (dd, J = 16.5, 10.0 Hz, 3H), 6.01 (d, J = 16.5 Hz, 3H), 5.90 (d, J = 10.0 Hz, 3H), 5.20 (s, 6H), 4.02 (s, 6H); ^{13}C NMR (151 MHz, DMSO-d_6) δ 166.7 (3C), 137.1 (3C), 127.0 (3C), 55.4 (3C), 43.9 (3C); IR (neat) ν_{max} (cm^{-1}) = 3277, 1651, 1533, 1410, 1240, 1195, 943; HRMS-ESI (m/z) [M + H]$^+$ calcd for $C_{15}H_{25}N_6O_9S_3$, 529.0840; found, 529.0862.

N,N′,N″-(Benzene-1,3,5-triyltris(methylene))triacrylamide (**Bz1**). To a solution of benzene-1,3,5-triyltrimethanamine (**6**, 250 mg, 1.51 mmol, 1 equiv) in MeCN (6 mL) and water (4 mL) was added NaOH (302 mg, 7.55 mmol, 5.0 equiv), and the mixture was cooled to 0 °C. Then, acryloyl chloride (440 uL, 5.44 mmol, 3.6 equiv) was added dropwise, and the reaction was allowed to go to room temperature, and stirring was continued for 4 h. After this time, MeCN was removed and the resulting mixture was extracted with EtOAc (twice). The combined organic layers were washed with brine, dried over Na_2SO_4, filtered, and concentrated in vacuo. The crude was purified by C18 reversed-phase column chromatography to obtain, after freeze-drying (from MeCN/water 1:1 and FA 0.1%), the title compound, which was isolated as a white amorphous solid (47 mg, 0.13 mmol, 10%): ^{1}H NMR (500 MHz, DMSO-d_6) δ 8.62 (t, J = 6.0 Hz, 3H), 7.04 (s, 3H), 6.26 (dd, J = 17.1, 10.1 Hz, 3H), 6.11 (dd, J = 17.1, 2.3 Hz, 3H), 5.61 (dd, J = 10.1, 2.2 Hz, 3H), 4.30 (d, J = 6.0 Hz, 6H); ^{13}C NMR (126 MHz, DMSO-d_6) δ 164.5 (3C), 139.6 (3C), 131.7 (3C), 125.5(3C), 125.2 (3C), 42.1 (3C); IR (neat) ν_{max} (cm^{-1}) = 3292, 1651, 1535, 1408, 1240, 1196, 945; HRMS-ESI (m/z) [M + Na]$^+$ calcd for $C_{18}H_{21}N_3NaO_3$, 350.1475; found, 350.1465.

N,N′,N″-(Benzene-1,3,5-triyltris(methylene))tris(2-chloroacetamide) (**Bz2**). Prepared according to general procedure A using benzene-1,3,5-triyltrimethanamine (**6**, 330 mg, 2 mmol), K_2CO_3 (1.24 g, 9 mmol), and chloroacetyl chloride (573 uL, 7.2 mmol). The title compound was isolated after trituration with EtOAc as a white amorphous solid (139 mg, 0.35 mmol, 18%): ^{1}H NMR (500 MHz, DMSO-d_6) δ 8.75 (t, J = 6.0 Hz, 3H), 7.05 (s, 3H), 4.26 (d, J = 5.9 Hz, 6H), 4.11 (s, 6H); ^{13}C NMR (126 MHz, DMSO-d_6) δ 166.0 (3C), 139.2 (3C), 125.0 (3C), 42.7 (3C), 42.4 (3C); IR (neat) ν_{max} (cm^{-1}) = 3292, 1649, 1535, 1408, 1238, 1196, 943; HRMS-ESI (m/z) [M + H]$^+$ calcd for $C_{15}H_{19}Cl_3N_3O_3$, 394.0487; found, 394.0506.

N,N′,N″-(Benzene-1,3,5-triyltris(methylene))-triethenesulfonamide (**Bz3**). Prepared according to general procedure B by treating a solution of 2-chloroethanesulfonyl chloride (1.25 mL, 11.9 mmol) and triethylamine (1.33 mL, 9.54 mmol) in CH_2Cl_2 (20 mL) with a solution of benzene-1,3,5-triyltrimethanamine (**6**,500 mg, 2.65 mmol) and triethylamine (1.21 mL, 8.75 mmol) in CH_2Cl_2 (10 mL). The crude was purified by flash chromatography using EtOAc/cyclohexane (2:1) as eluent to obtain the title compound as a yellowish oil (24 mg, 0.055 mmol, 2.1%): R_f =0.18 (EtOAc/cyclohexane 2:1); ^{1}H NMR (500 MHz, chloroform-d) δ 7.21 (s, 3H), 6.54 (dd, J = 16.5, 9.9 Hz, 3H), 6.25 (d, J = 16.5 Hz, 3H), 5.99 (d, J = 9.9 Hz, 3H), 5.29 (t, J = 6.6 Hz, 3H), 4.08 (d, J = 6.4 Hz, 6H); ^{13}C NMR (126 MHz, $CDCl_3$) δ 138.1 (3C), 135.7 (3C), 127.6 (3C), 127.4 (3C), 46.6 (3C); IR (neat) ν_{max} (cm^{-1}) = 3277, 1643, 1535, 1427, 1317, 1142, 946; HRMS-ESI (m/z) [M + H]$^+$ calcd for $C_{15}H_{22}N_3O_6S_3$, 436.0665; found, 436.0693.

Protein Expression and Purification. The expression vector pGEX-4t-3 carrying the coding sequence was transformed into *E. coli* BL21-Gold (DE3). A 2 L TB culture was incubated at 37 °C to OD_{600} = 1; then protein expression was induced by addition of 0.5 mM IPTG and performed overnight at 20 °C. Cells were harvested by centrifugation, resuspended in lysis buffer (50 mM Tris, pH 7.4, 500 mM NaCl, 0.5 mM PMSF, and 2 mM DTT), and disrupted using a microfluidizer (three rounds). The cell lysate was cleared by centrifugation (20 000 rpm, 4 °C, 60 min). GST-tagged **K1** was isolated from the supernatant by affinity chromatography (Aekta Pure, GSTPrep FF 16/10, GE Healthcare, 4 °C). After being loaded, the column was washed with wash buffer (50 mM Tris, pH 7.4, 100 mM NaCl, 2 mM DTT) until baseline (OD_{280}) was reached. PreScission (His-tagged) cleavage was performed on the column overnight at 4 °C in wash buffer. Protein **K1** was eluted with wash buffer and incubated with Ni-NTA agarose resin (10 min, rt). After removal of the resin by centrifugation, the target protein was concentrated via ultrafiltration to approximately 9 mg mL^{-1} (Amicon, Merck, 3 kDa MWCO, rt). Subsequent size-exclusion chromatography was performed (Aekta Pure, Column HiLoad 16/600 Superdex 75 pg, GE Healthcare in 25 mM HEPES, pH 7.4, 100 mM NaCl, 0.5 mM TCEP). Purified **K1** was concentrated (Amicon, Merck, 3 kDa MWCO, rt) to approximately 2−5 mg mL^{-1}, snap frozen, and stored at −80 °C. Generated vector constructs were sequence proven by Sanger sequencing and protein purity confirmed via SDS-PAGE.

Protein Modification with Tris-Electrophiles. For time- and pH-dependent analysis of product formation, 50 μM **K1** was incubated with 1 mM tris-electrophile (100 mM in DMSO) in cross-linking buffer (50 mM HEPES, 50 mM NaCl, pH 6.5, 7.5 or 8.5) at 25 °C and 350 rpm. At time points of t = 0, 1, 3, and 5 h, the reaction was quenched with a final concentration of 1% TFA. Analysis was performed on a 1290 Infinity coupled to a 6120 quadrupole LC/MS (Agilent Technologies) using a Zorbax Eclipse XDB-C18 reversed-phase column (4.6 × 150 mm, particle size 5 μm, Agilent Technologies) and a linear gradient of 10−60% B in 10 min (solvent A: H_2O + 0.1% TFA; solvent B: acetonitrile + 0.1% TFA; flow rate of 1 mL min^{-1}). MS spectra were obtained with solvents containing 0.1% formic acid and 0.01% TFA. For **K1** + **Bz3**, the gradient was adjusted to 10−80% B in 10 min. For full conversion of protein, 50 μM **K1** was incubated with 1 mM tris-electrophile (stock solution: 100 mM in DMSO) in cross-linking buffer (50 mM HEPES, pH 8.5, 50 mM NaCl) at 350 rpm. Depending on the tris-electrophile, the incubation time and temperature were adjusted (for details, see Table S1). A buffer exchange was performed using Vivaspin 500 centrifugal concentrators (3 kDa MWCO, rt) before measurements.

Circular Dichroism Spectroscopy. All CD and thermal stability measurements were performed with 2 μM protein in buffer (5 mM sodium phosphate, pH 7.4, 20 °C) using a cuvette with 10 mm optical path length. Measurements were performed on a Jasco J-1500 CD spectrometer equipped with a Jasco CTU-100 temperature control unit. CD spectra were recorded using the following settings: λ = 260−195 nm, DIT = 2 s, bandwidth = 1 nm, scanning speed = 100 nm min^{-1} (10 accumulations). Molar ellipticity at λ = 222 nm ($[\theta]_{222}$/deg cm^2 dmol^{-1}) was calculated[32] using background-corrected CD signals and the equation

$$[\theta]_{222} = \frac{\theta_{222}^{raw}}{cnL}$$

where θ_{222}^{raw} is ellipticity (mdeg) at λ = 222 nm, c is the molar concentration of the protein (mol L^{-1}), n is the number of amino acids in the protein, and L is the path length of the cuvette (mm). The helical content (or helicity/%) was determined using the so-called "222 nm method"[32] with the equation

$$\text{helical content} = \frac{[\theta]_{222} + [\theta]_{222}^{0}}{[\theta]_{222}^{100} + [\theta]_{222}^{0}} \times 100$$

where $[\theta]_{222}^{0}$ = −3000 deg cm^2 dmol^{-1} and $[\theta]_{222}^{100}$ = −39 500 deg cm^2 dmol^{-1} at λ = 222 nm and correspond to the estimated ellipticity for a protein with 0 and 100% helical content, respectively. For thermal stability measurements, the following settings were used: λ = 222 nm, temperature range = 20−98 °C, heating rate = 1 °C min^{-1} (with 1 °C increments), DIT = 2 s, bandwidth = 1 nm. Jasco spectra analysis software (version 2.15.09) was used to determine the melting temperature (T_m). Smoothing (convolution width = 21) and first derivative calculations (convolution width = 11) were performed using the Savitzky−Golay algorithm, and the resulting peak maxima were determined.

■ ASSOCIATED CONTENT

Supporting Information

The Supporting Information is available free of charge at https://pubs.acs.org/doi/10.1021/acs.joc.9b02490.

DOI: 10.1021/acs.joc.9b02490
J. Org. Chem. 2020, 85, 1476−1483

NMR spectra of tris-electrophiles, HPLC chromatograms of protein cross-linking reactions, and MS spectra, CD spectra and CD melting curves of cross-linked proteins (PDF)

AUTHOR INFORMATION

Corresponding Authors

*E-mail: s.n.neubacher@vu.nl.
*E-mail: t.n.grossmann@vu.nl.

ORCID

Tom N. Grossmann: 0000-0003-0179-4116

Notes

The authors declare the following competing financial interest(s): S.N. and T.N.G. are listed as an inventor on a patent application related to the INCYPRO stabilization approach.

ACKNOWLEDGMENTS

We thank the European Research Council (ERC Starting Grant No. 678623; ERC proof-of-concept, No. 839088).

REFERENCES

(1) Bornscheuer, U. T.; Huisman, G. W.; Kazlauskas, R. J.; Lutz, S.; Moore, J. C.; Robins, K. Engineering the third wave of biocatalysis. *Nature* **2012**, *485*, 185−194.

(2) Hackenberger, C. P. R.; Schwarzer, D. Chemoselective ligation and modification strategies for peptides and proteins. *Angew. Chem., Int. Ed.* **2008**, *47*, 10030−10074.

(3) Sali, A.; Shakhnovich, E.; Karplus, M. How does a protein fold. *Nature* **1994**, *369*, 248−251.

(4) Reetz, M. T. The importance of additive and non-additive mutational effects in protein engineering. *Angew. Chem., Int. Ed.* **2013**, *52*, 2658−2666.

(5) Jost, C.; Pluckthun, A. Engineered proteins with desired specificity: Darpins, other alternative scaffolds and bispecific IgGs. *Curr. Opin. Struct. Biol.* **2014**, *27*, 102−112.

(6) Magliery, T. J. Protein stability: Computation, sequence statistics, and new experimental methods. *Curr. Opin. Struct. Biol.* **2015**, *33*, 161−168.

(7) Chapman, A. M.; McNaughton, B. R. Scratching the surface: Resurfacing proteins to endow new properties and function. *Cell Chem. Biol.* **2016**, *23*, 543−553.

(8) Agostini, F.; Voller, J. S.; Koksch, B.; Acevedo-Rocha, C. G.; Kubyshkin, V.; Budisa, N. Biocatalysis with unnatural amino acids: Enzymology meets xenobiology. *Angew. Chem., Int. Ed.* **2017**, *56*, 9680−9703.

(9) Martinez-Saez, N.; Sun, S.; Oldrini, D.; Sormanni, P.; Boutureira, O.; Carboni, F.; Companon, I.; Deery, M. J.; Vendruscolo, M.; Corzana, F.; Adamo, R.; Bernardes, G. J. L. Oxetane grafts installed site-selectively on native disulfides to enhance protein stability and activity invivo. *Angew. Chem., Int. Ed.* **2017**, *56*, 14963−14967.

(10) Camarero, J. A.; Muir, T. W. Biosynthesis of a head-to-tail cyclized protein with improved biological activity. *J. Am. Chem. Soc.* **1999**, *121*, 5597−5598.

(11) Iwai, H.; Pluckthun, A. Circular beta-lactamase: Stability enhancement by cyclizing the backbone. *FEBS Lett.* **1999**, *459*, 166−172.

(12) Schoene, C.; Fierer, J. O.; Bennett, S. P.; Howarth, M. Spytag/spycatcher cyclization confers resilience to boiling on a mesophilic enzyme. *Angew. Chem., Int. Ed.* **2014**, *53*, 6101−6104.

(13) Moore, E. J.; Zorine, D.; Hansen, W. A.; Khare, S. D.; Fasan, R. Enzyme stabilization via computationally guided protein stapling. *Proc. Natl. Acad. Sci. U. S. A.* **2017**, *114*, 12472−12477.

(14) Liu, T.; Wang, Y.; Luo, X. Z.; Li, J.; Reed, S. A.; Xiao, H.; Young, T. S.; Schultz, P. G. Enhancing protein stability with extended disulfide bonds. *Proc. Natl. Acad. Sci. U. S. A.* **2016**, *113*, 5910−5915.

(15) Luhmann, T.; Mong, S. K.; Simon, M. D.; Meinel, L.; Pentelute, B. L. A perfluoroaromatic abiotic analog of h2 relaxin enabled by rapid flow-based peptide synthesis. *Org. Biomol. Chem.* **2016**, *14*, 3345−3349.

(16) Pelay-Gimeno, M.; Glas, A.; Koch, O.; Grossmann, T. N. Structure-based design of inhibitors of protein-protein interactions: Mimicking peptide binding epitopes. *Angew. Chem., Int. Ed.* **2015**, *54*, 8896−8927.

(17) Kent, S. B. H. Novel protein science enabled by total chemical synthesis. *Protein Sci.* **2019**, *28*, 313−328.

(18) Dani, V. S.; Ramakrishnan, C.; Varadarajan, R. MODIP revisited: Re-evaluation and refinement of an automated procedure for modeling of disulfide bonds in proteins. *Protein Eng., Des. Sel.* **2003**, *16*, 187−193.

(19) Pelay-Gimeno, M.; Bange, T.; Hennig, S.; Grossmann, T. N. In situ cyclization of native proteins: Structure-based design of a bicyclic enzyme. *Angew. Chem., Int. Ed.* **2018**, *57*, 11164−11170.

(20) http://www.molinspiration.com (accessed September 1, 2019).

(21) Ohtoyo, M.; Machinaga, N.; Inoue, R.; Hagihara, K.; Yuita, H.; Tamura, M.; Hashimoto, R.; Chiba, J.; Muro, F.; Watanabe, J.; Kobayashi, Y.; Abe, K.; Kita, Y.; Nagasaki, M.; Shimozato, T. Component of caramel food coloring, thi, causes lymphopenia indirectly via a key metabolic intermediate. *Cell Chem. Biol.* **2016**, *23*, 555−560.

(22) Brauckhoff, N.; Hahne, G.; Yeh, J. T. H.; Grossmann, T. N. Protein-templated peptide ligation. *Angew. Chem., Int. Ed.* **2014**, *53*, 4337−4340.

(23) Chen, S. Y.; Morales-Sanfrutos, J.; Angelini, A.; Cutting, B.; Heinis, C. Structurally diverse cyclisation linkers impose different backbone conformations in bicyclic peptides. *ChemBioChem* **2012**, *13*, 1032−1038.

(24) Vistoli, G.; Pedretti, A.; Testa, B. Partition coefficient and molecular flexibility: The concept of lipophilicity space. *Chem. Biodiversity* **2009**, *6*, 1152−1169.

(25) Mancuso, L.; Knobloch, T.; Buchholz, J.; Hartwig, J.; Moller, L.; Seidel, K.; Collisi, W.; Sasse, F.; Kirschning, A. Preparation of thermocleavable conjugates based on ansamitocin and superparamagnetic nanostructured particles by a chemobiosynthetic approach. *Chem. - Eur. J.* **2014**, *20*, 17541−17551.

(26) Granzhan, A.; Schouwey, C.; Riis-Johannessen, T.; Scopelliti, R.; Severin, K. Connection of metallamacrocycles via dynamic covalent chemistry: A versatile method for the synthesis of molecular cages. *J. Am. Chem. Soc.* **2011**, *133*, 7106−7115.

(27) van de Langemheen, H.; Korotkovs, V.; Bijl, J.; Wilson, C.; Kale, S. S.; Heinis, C.; Liskamp, R. M. J. Polar hinges as functionalized conformational constraints in (bi)cyclic peptides. *ChemBioChem* **2017**, *18*, 387−395.

(28) Sinha, J.; Podgorski, M.; Huang, S. J.; Bowman, C. N. Multifunctional monomers based on vinyl sulfonates and vinyl sulfonamides for crosslinking thiol-michael polymerizations: Monomer reactivity and mechanical behavior. *Chem. Commun.* **2018**, *54*, 3034−3037.

(29) Tam-Chang, S. W.; Stehouwer, J. S.; Hao, J. S. Formation of a macrobicyclic tris(disulfide) by molecular self-assembly. *J. Org. Chem.* **1999**, *64*, 334−335.

(30) De Guzman, R. N.; Goto, N. K.; Dyson, H. J.; Wright, P. E. Structural basis for cooperative transcription factor binding to the cbp coactivator. *J. Mol. Biol.* **2006**, *355*, 1005−1013.

(31) Stiller, C.; Kruger, D. M.; Brauckhoff, N.; Schmidt, M.; Janning, P.; Salamon, H.; Grossmann, T. N. Translocation of an intracellular protein via peptide-directed ligation. *ACS Chem. Biol.* **2017**, *12*, 504−509.

(32) Wei, Y.; Thyparambil, A. A.; Latour, R. A. Protein helical structure determination using CD spectroscopy for solutions with strong background absorbance from 190 to 230 nm. *Biochim. Biophys. Acta, Proteins Proteomics* **2014**, *1844* (12), 2331.

DOI: 10.1021/acs.joc.9b02490
J. Org. Chem. 2020, 85, 1476−1483